Murali, K., Sparkes, H., Pandiyan, B. V., & Prasad, K. J. R. (2017). Synthesis, photophysical properties and DFT analysis of highly substituted pyrido carbazole-based "push pull" chromophores. *New Journal of Chemistry*, *41*(16), 8242-8252. https://doi.org/10.1039/c7nj00643h

Synthesis, Photophysical Properties and DFT analysis of Highly substituted Pyrido Carbazole-based "push pull" chromophores

Karunanidhi Murali [a], Hazel A. Sparkes [b], Baskaran Vijaya Pandiyan [c],

Karnam Jayarampillai Rajendra Prasad [a*]

[a*] Department of Chemistry, Bharathiar University, Coimbatore 641046, India.

[b] School of Chemistry, University of Bristol, Cantock's Close, Bristol, BS8 1TS, United Kingdom.

[c] Department of Physics, Bharathiar University, Coimbatore 641046, India.

Abstract

A series of new fluorscent pyrido[2,3-*a*]carbazole derivatives were synthesized in excellent yield through an efficient and single step strategy based on a four-component reaction with 2,3,4,9-tetrahydro-1*H*-carbazol-1-one, malononitrile, and aryl/heteroaryl aldehydes as synthetic inputs and sodium ethoxide (NaOEt) as a catalyst in methanol under reflux condition. The structures of the compounds were established by FT-IR, ^{1}H NMR, ^{13}C NMR, X-ray diffraction and elemental analysis. The photophysical features of the synthesized compounds **5** (**a-q**) containing "push-pull" scaffolds are investigated and reported with the aim of achieving good fluorescent materials. The UV-vis absorption and fluorescence emission of the compounds were studied in solvents of varying polarities and showed an increase in the solvent polarity led to an increase in the Stokes shift. This study revealed that the investigated compounds are highly fluorescent molecules (**φ_{fl} = 0.27-0.65**) with lifetimes in the range **7-9 ns**. Furthermore, we analyzed for band gap energy associated with HOMO-LUMO, through DFT studies.

Keywords

Pyrido[2,3-*a*]carbazole

Malononitrile

Donor-acceptor systems

Fluorescence quantum yield

Fluorescence lifetime

DFT calculations

---

*Corresponding author e-mail: prasad_125@yahoo.com, Tel: +91-422-2422311, Fax: +91-422-2422387

1. Introduction

Development of organic fluorescent heterocyclic compounds has been the subject of intense study because of its rapidly expanding applications in molecular probes,[1] non-linear optics (NLO),[2] fluorescent makers,[3] organic light emitting diodes (OLED),[4] photovoltaic cells[5] and in traditional textile and polymer field.[6] Organic compounds containing both electron donating (D) and accepting (A) substituents in a single molecule, exhibit interesting optical and spectral properties due to intramolecular charge transfer (ICT). This phenomenon has long been a topic of great interest in photochemistry owing to fundamental scientific value[7] as well as potential applications in photoelectronic and nonlinear optical devices,[8,9] and understanding photochemical and photobiological processes.[10] ICT is particularly important in fluorescent compounds which act as polarity probes or ionophores.[11]

Organic molecules with large delocalized π-electron systems have attracted significant interest due to potential applications associated with strong emission behavior and large nonlinear optical properties.[12-14] The presence and nature of electron donating and accepting groups play significant roles in such properties. Compounds of this class show solvent polarity dependent changes in their photophysical properties such as fluorescence quantum yield, maximum emission wavelength and fluorescence lifetime. In past decades, the donor-π-acceptor molecules have been extensively used for second order NLO applications due to their high β hyper polarizability.

Carbazole is a nitrogen containing π-conjugated heterocyclic unit that has interesting optical and electronic properties such as photoconductivity and photorefractivity.[15,16] Carbazole-based compounds are known for their intense luminescence[17,18] and widely used on OLEDs as emitters. Carbazole is well known for its electron donating properties[19] and incorporation of some electron withdrawing groups on carbazole raise the highest occupied molecular orbital (HOMO) energy levels and reduce the barrier height for hole injection. The introduction of additional heterocyclic structure in to the donor moiety of chromophores could dramatically influence the chromophores' hyper polarizability.[20] Due to the high electron affinity, pyridines are excellent candidates for incoporation as electron-withdrawing groups in push-pull scaffolds favoring intramolecular charge transfer (ICT). Su, *et al*.[21] showed that the combination of a carbazole electron-donor and a pyridine electron-acceptor could give bipolar host materials; for example, 2,6-bis[(3-(carbazol-9-yl)phenyl)]pyridine and 3,5-bis[(3-(carbazol-9-

yl)phenyl)]pyridine. These host materials were doped with iridium(III) bis[(4,6-(difluorophenyl)pyridinato-*N*,C2')]picolinate to create phosphorescent OLEDs. Dailey, *et al.* described the poly(2,5-pyridinediyl) (PPY) as an efficient electron transport layer in bilayer polymeric LEDs. The OLEDs with a PPY layer exhibited an external quantum efficiency 60-times greater than that of similar devices without a PPY layer.[22]

Heterocyclic substituents such as thiophene and oligomers [23-25] and combined thiophene-isophorone[26] in chromophores have enhanced nonlinearities and improved stability. Thiophene, in particular, is an appealing class of linkers in optoelectronics and influencing magnitude of the bandgap which induces ICT.[27,28] A derivative with methoxy substitution is of great importance to achieve high thermal stability and nonlinear optical response.[29] However, it is difficult to synthesize pyrido annulated carbazole compounds with D-π-A structure, because it requires multistep synthetic procedure, harsh reaction conditions and expensive starting material or catalyst.[30]

In this paper, we report the synthesis and photophysical properties of pyridocarbazole based push-pull scaffolds containing methoxy group as a donor and cyano group as an acceptor with aryl/heteroaryl substituents at C-4 position through an efficient one-pot strategy. We disclose here full details and discussion of synthetic approaches, structural characteristics and fluorescent responses using both solvatochromic shift method and theoretical method.

2. Results and discussion

2.1. Chemistry

The reaction of 2,3,4,9-tetrahydro-1*H*-carbazol-1-one (**1**), malononitrile (**2**) and aryl/heteroaryl aldehydes (**3**) in the presence of a catalytic amount of sodium ethoxide (NaOEt) under reflux in methanol targeting pyrano[2,3-*a*] carbazole **4** as the product. On the basis of spectral data and X-ray diffraction the structure **4** was easily ruled out and these data indicate the formation of structure **5** as the product (**Scheme 1**).

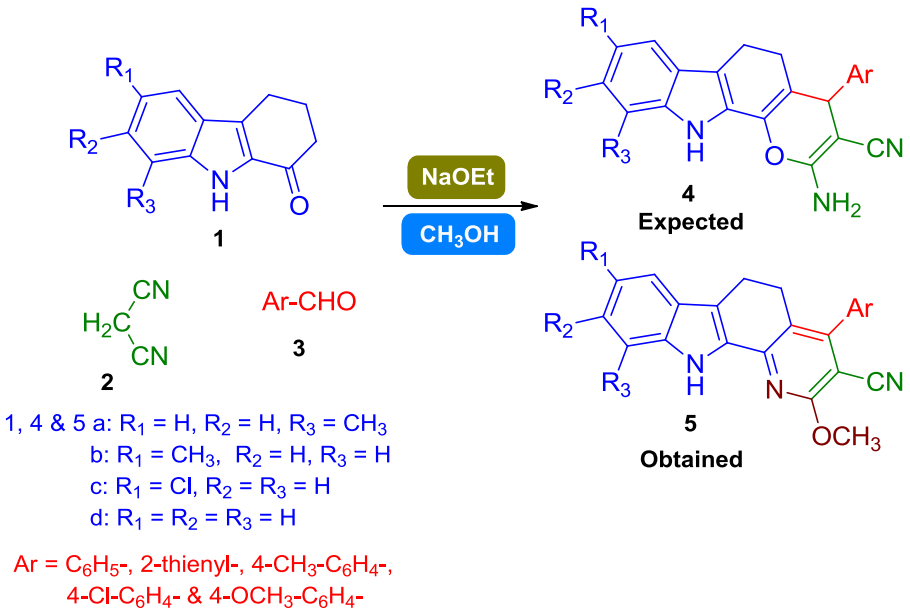

Scheme 1. Synthesis of 2-methoxy-4-aryl/heteroaryl-pyrido[2,3-*a*]carbazole-3-carbonitrile.

In our initial endeavour, we investigated the reaction of 8-methyl-2,3,4,9-tetrahydro-1*H*-carbazol-1-one **1a** with malononitrile **2** and benzaldehyde **3a** using various base catalysts in methanol (**Scheme 2** and **Table.1**).

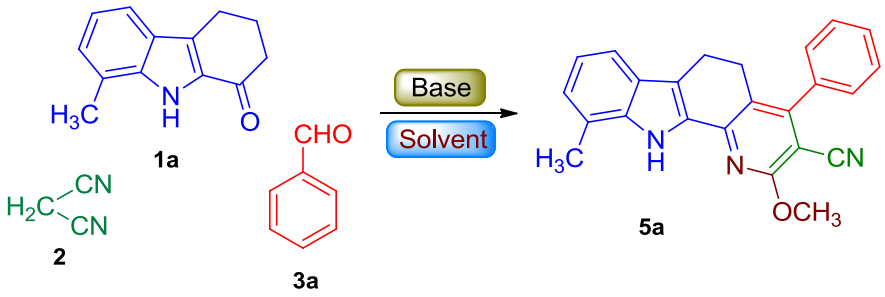

Scheme 2. Synthesis of novel pyrido[2,3-*a*]carbazole **5a**

Table.1 Optimization of reaction conditions of **5a**[a]

Entry	Solvent	Base	Temperature (°C)	Time (h)	Yield[b]
1	MeOH	-	RT	12	-
2.	MeOH	-	60	12	-
3.	MeOH	Et_3N	60	8	58
4.	MeOH	DABCO	60	8	50
5.	MeOH	NaOH	65	8	63
6.	MeOH	KOH	65	8	67

7.	MeOH	NaOEt	70	3	78
8.	MeOH	NaOEt	80	3	85
9.	MeOH	Piperidine	80	5	55

[a] The reaction was performed with **1a** (1.0 mmol), malononitrile **2** (1.0 mmol) and benzaldehyde **3** (1.0 mmol) using NaOEt (0.023g in 1mL EtOH) under MeOH reflux. [b] Isolated yields, -Trace product.

The effects of a variety of organic bases on the reaction efficiency and yield were screened. In the absence of catalyst, we did not observe any of the four-component products both at room temperature and reflux conditions even after 12 h stirring in methanol (Table 1, entries 1-2). Interestingly, when the same reaction was carried out in the presence of catalytic amounts of Et_3N and DABCO in refluxing methanol the desired four-component product **5a** was obtained in moderate yields (entries 3-4). Encouraged by these results we attempted to optimize this reaction by using different bases such as NaOH, KOH, NaOEt and piperidine. Among all these, NaOEt was found to be optimum base for this domino transformation, where a yield of 85% of the product **5a** was obtained in 3 h (entry 8). Finally, the optimum reaction temperatures was also examined and find that the reaction proceeded smoothly and that almost complete conversion of reactants was observed at 80 ℃ to afford the desired product **5a**.

The structures of all new compounds were fully characterized by spectroscopic techniques. For example, the FT-IR spectrum of compound **5a** revealed the absence of any band due to a carbonyl functional group. The prominent absorptions at 3337 and 1556 cm^{-1} were due to the presence of indole NH and C=N groups respectively. The cyano group (CN) stretching vibration was assigned to a strong band at 2217 cm^{-1}. The ^1H NMR spectrum showed a broad singlet at δ 8.65 ppm due to indole NH. The signals due to C_9, C_8 and C_7 protons appeared as a multiplet in the region of δ 7.52-7.44 ppm while the C'_4 proton accounted for a multiplet signal centered at δ 7.42 ppm. The signals due to C'_6, C'_2, C'_5 & C'_3 protons were visible as two multiplets in the region δ 7.34-7.31 and 7.10-7.04 ppm, and three protons from the methoxy group resonated as a singlet at δ 4.18 ppm. Methylene protons of C_6 and C_5 appeared as two multiplets centered at δ 2.94 and δ 2.85 ppm respectively. A singlet at δ 2.57 ppm accounted for the three methyl protons at C_{10} position. The ^{13}C NMR spectrum of **5a** displayed 24 resonances in agreement with the proposed structure. The resonance signals at δ 117.5 and 54.4 ppm were attributed to cyano and methoxy carbons respectively. The exact mass of **5a** observed as a 365.1525, which is very close

to its theoretical value of 366.1530 $(C_{24}H_{19}N_3O)^+$. Further, **5a** was confirmed unambiguously by a single crystal X-ray diffraction (**Fig. 1**).

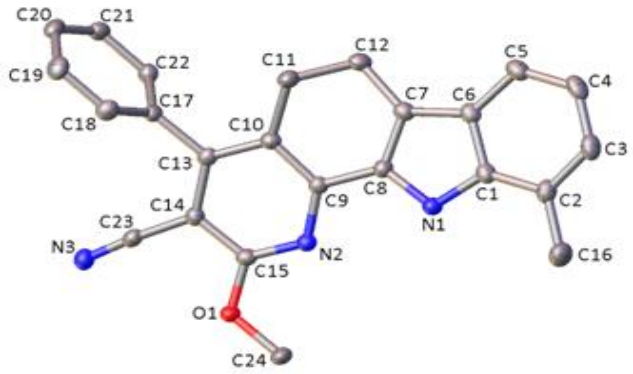

Fig. 1. X-ray crystal structure of **5a** with ellipsoids depicted at the 50% probability level and atomic labeling shown. Hydrogen atoms are omitted for clarity.

To generalize this methodology, we subjected a series of other aryl and heteroaryl aldehydes having electron-donating as well as electron-withdrawing substituents to obtain the corresponding 2-methoxy-4-aryl/heteroaryl-5,6-dihydro-11*H*-pyrido[2,3-*a*]carbazole-3 carbonitriles **5** (**b**-**q**). It is note worthy that there is no reaction with aliphatic aldehydes under similar condition (entries **18** and **19**) and the results are presented in **Table 2**. The structures of the synthesized compounds were consistent with their FT-IR, ^{1}H NMR, and ^{13}C NMR spectra, elemental analysis and single crystal X-ray diffraction. In general, the reactions were clean and no side products were detected.

Table 2. Scope of various substituted pyrido[2,3-*a*]carbazole derivatives **5** (**a-q**).

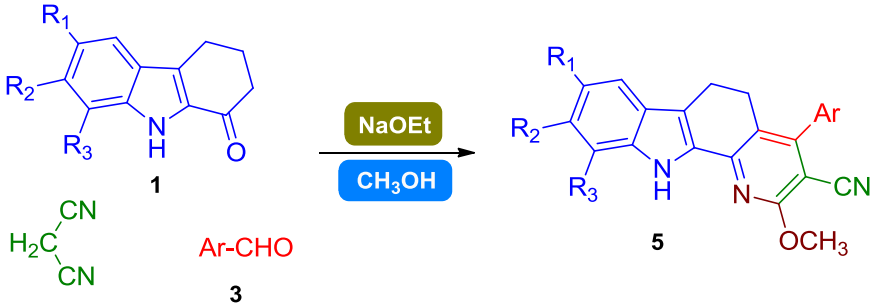

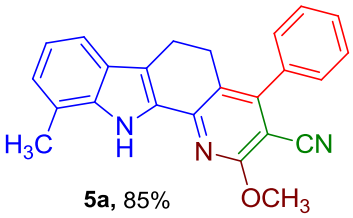 **5a**, 85%	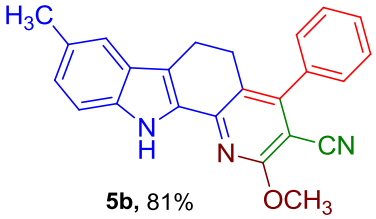 **5b**, 81%	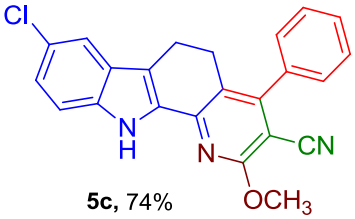 **5c**, 74%
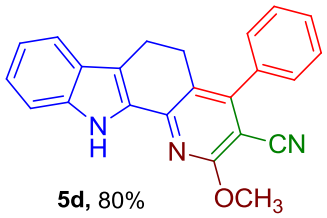 **5d**, 80%	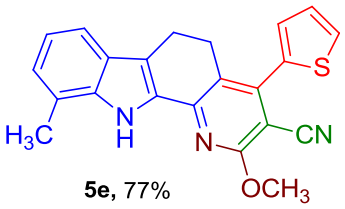 **5e**, 77%	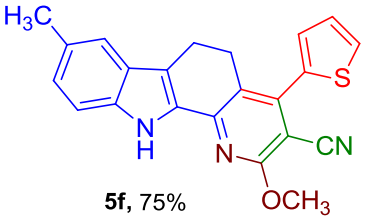 **5f**, 75%
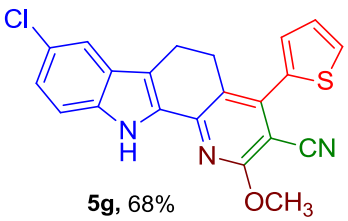 **5g**, 68%	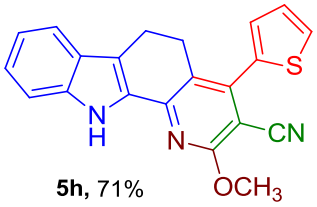 **5h**, 71%	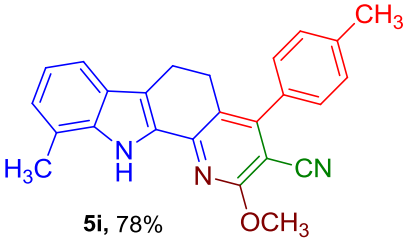 **5i**, 78%
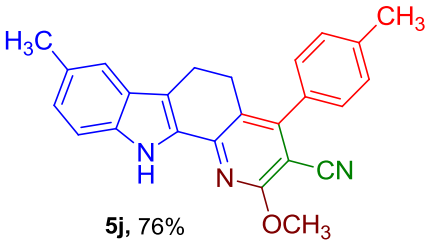 **5j**, 76%	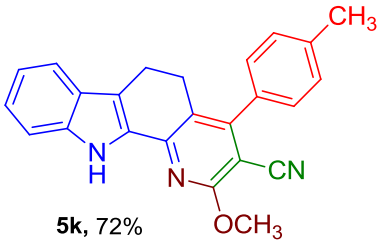 **5k**, 72%	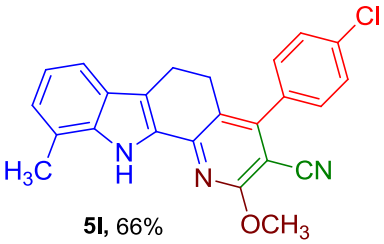 **5l**, 66%
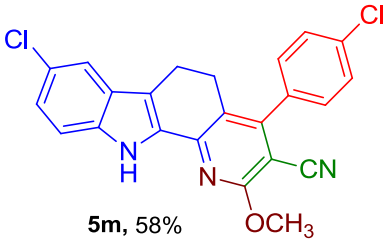 **5m**, 58%	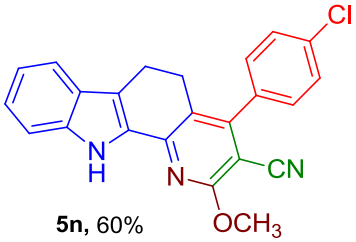 **5n**, 60%	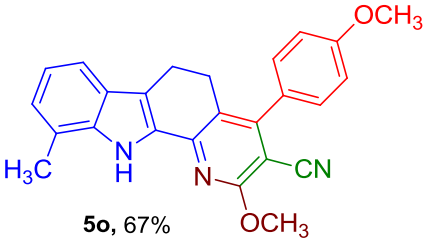 **5o**, 67%

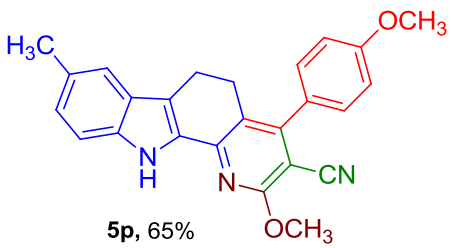

5p, 65%

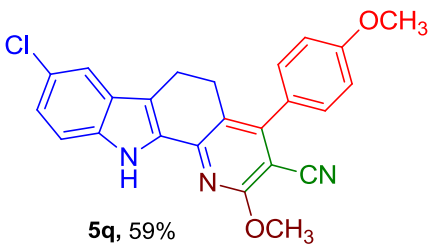

5q, 59%

2.2. Single Crystal X-ray Diffraction

X-ray diffraction experiments for **5a**, **5d**, **5h**, **5j** and **5k** were carried out at 100(2) K on a Bruker APEX II diffractometer with CCD area detector using Mo-K_α radiation (λ = 0.71073 Å). Intensities were integrated[31] and absorption corrections were carried out based on equivalent reflections using SADABS.[32] All of the structures were solved using superflip,[33] all of the structures were refined against F^2 in SHELXL[34] using Olex2.[35] All of the non-hydrogen atoms were refined anisotropically. While all of the hydrogen atoms were located geometrically and refined using a riding model, with the exception of the N-H in **5a, 5h** and **5j** which were located in the difference map and refined freely. The CCDC numbers are 1498651-1498655. The crystal structure of compounds **5d**, **5h**, **5j** and **5k** are shown in **Figs.2-5**.

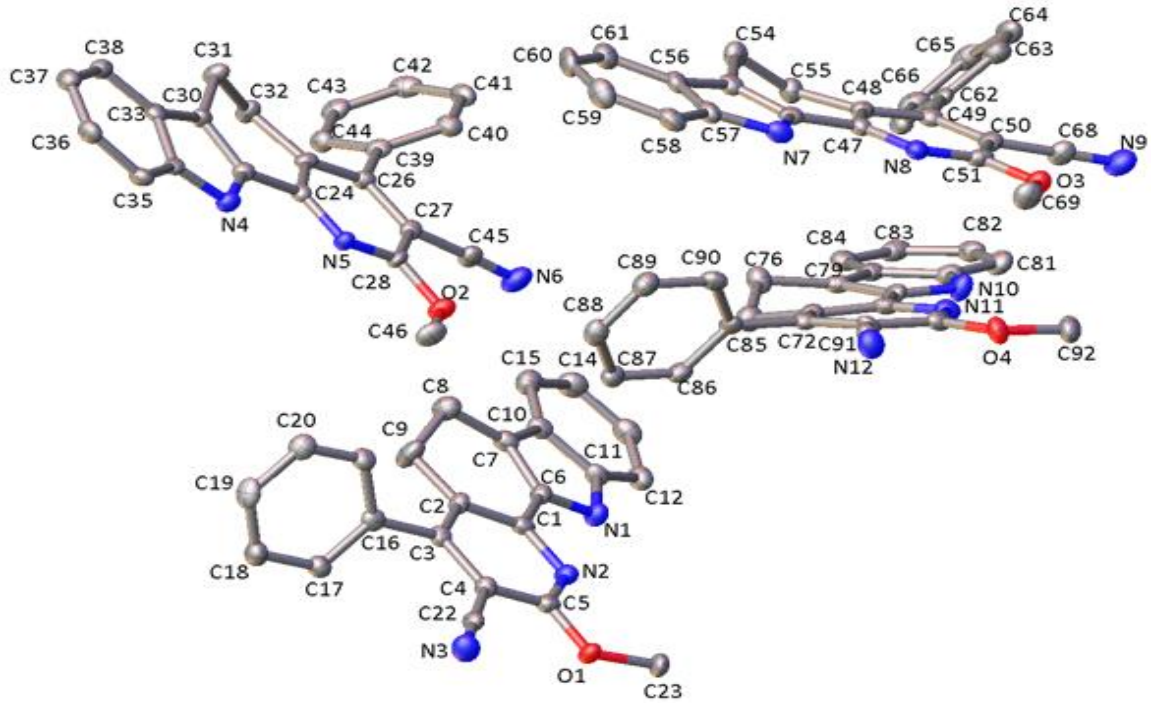

Fig.2. X-ray crystal **s**tructure of **5d** with ellipsoids depicted at the 50% probability level and atomic labeling shown. Hydrogen atoms are omitted for clarity.

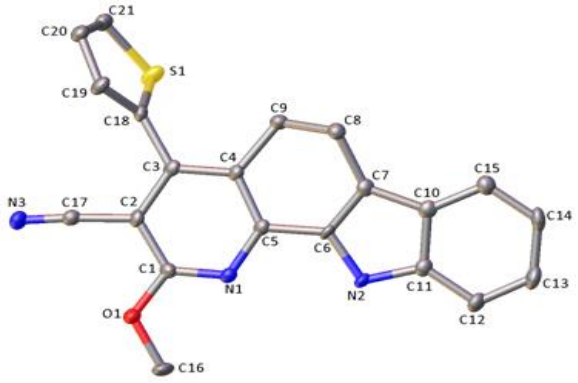

Fig.3. X-ray crystal structure of **5h** with ellipsoids depicted at the 50% probability level and atomic labeling shown. Hydrogen atoms are omitted for clarity.

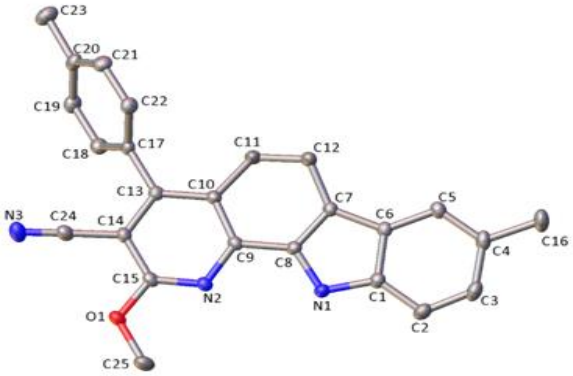

Fig.4. X-ray crystal structure of **5j** with ellipsoids depicted at the 50% probability level and atomic labeling shown. Hydrogen atoms are omitted for clarity.

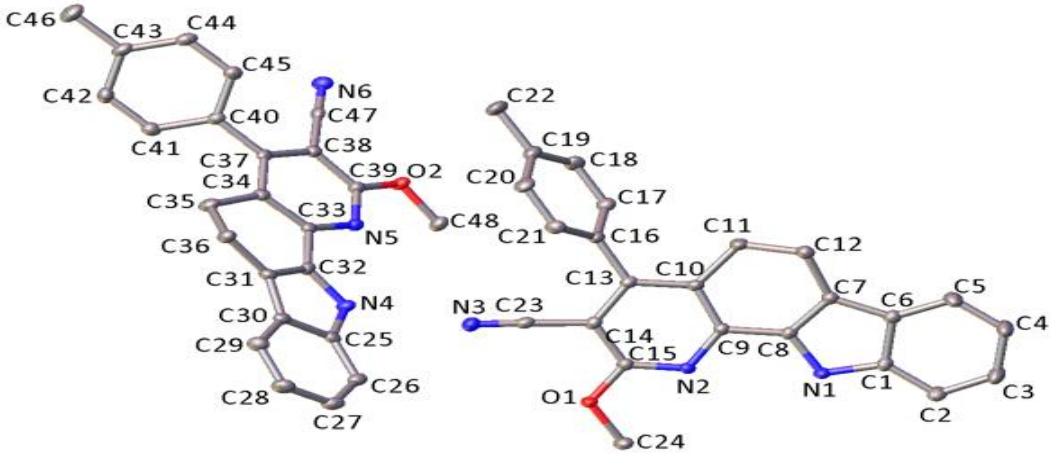

Fig.5. X-ray crystal structure of **5k** with ellipsoids depicted at the 50% probability level and atomic labeling shown. Hydrogen atoms are omitted for clarity.

A plausible mechanism for the formation of compound **5** is depicted in **Scheme 3**. Initially, the aryl / heteroaryl aldehyde undergoes Knoevenagel condensation with malononitrile

in the presence of base to give arylidene / heteroarylidene malononitrile **I**. The subsequent base promoted 1,4-Michael addition of intermediate **II** derived from 2,3,4,9-tetrahydro-1*H*-carbazol-1-one (**1**), affords the dinitrile intermediate **III** followed by prototropic shift and methanol addition to form an imino intermediate **V** through **t**he intermediate **IV** . Then **V** undergoes cyclization followed by dehydration and aerial oxidation to yield the final product **5**. The formation of the expected product pyranocarbazole **4** from the intermediate **IV** is ruled out because of the more stability of the observed aromatic product **5** than the unstable pyrano product **4**.

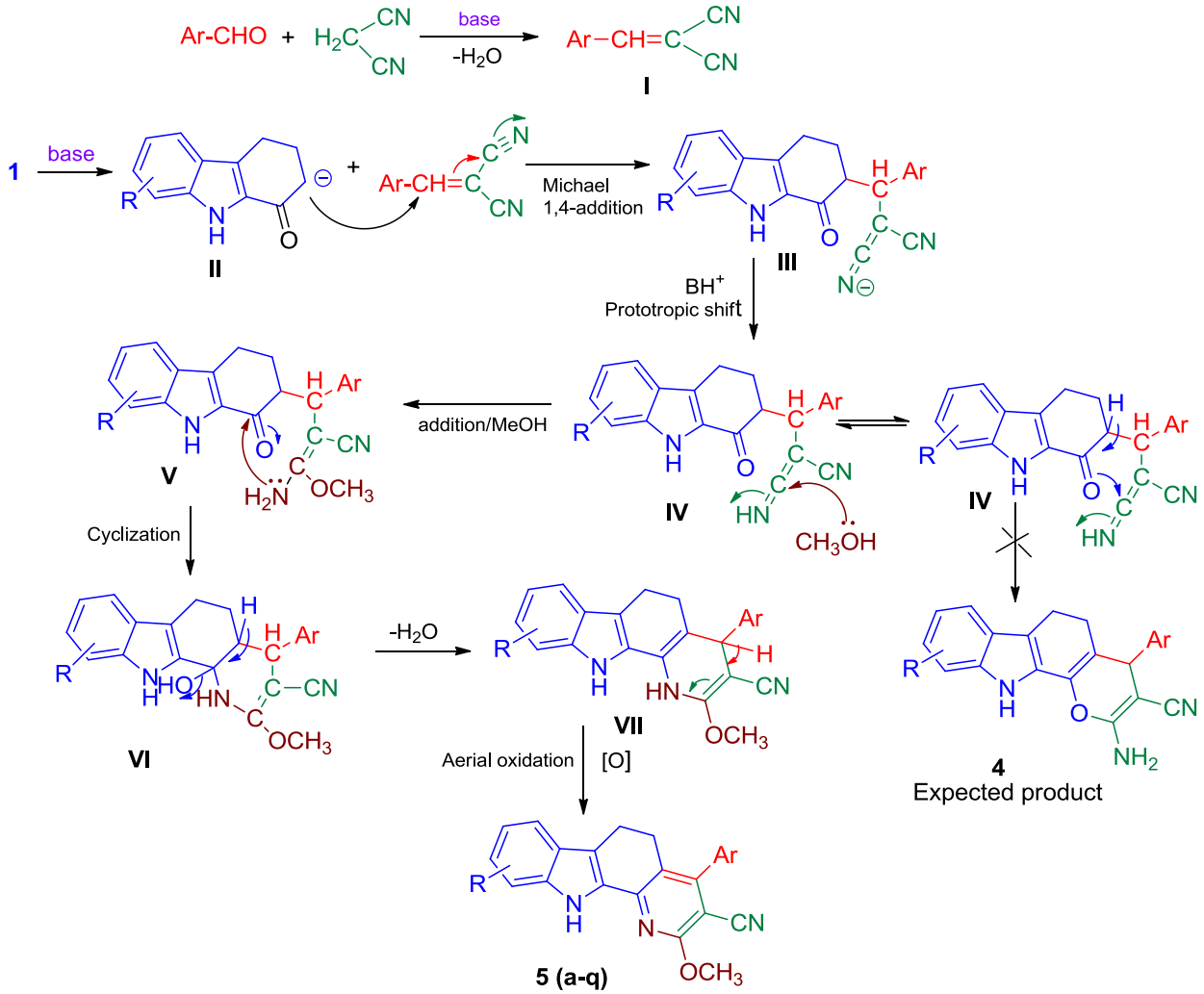

Scheme 3. Machanistic rationalization for the formation of **4** and **5**

2.3. Photophysical properties

Table 4 provides data from the photophysical characterization of the synthesized compounds **5** (**a-q**). The main purpose of evaluating the photophysical properties of these compounds was (i) to evaluate the effect of varying the donor or acceptor strength of the aryl/heteroaryl groups at the C-4 position of the pyrido[2,3-a]carbazole chromophore (ii) evaluating any solvatochromic effects in the absorption and emission spectra, so the photophysical characteristics of each molecule were evaluated in a series of organic solvents such as dichloromethane (DCM), chloroform ($CHCl_3$), methanol (MeOH) and N,N-dimethylformamide (DMF) with different polarities. The UV-vis absorption and emission spectra of compounds **5** (**a-q**) were studied in the range of 200-500 nm (λ_{abs}) and 400-700 nm (λ_{em}), respectively. Further, the fluorescence quantum yield of each compounds were also determined by the standard literature method using Rhodamine-6G as a reference standard.[36-38] The absorption (λ_{abs}), emission (λ_{emi}) spectra, quantum yield (φ_{fl}) and Stokes shifts values in different solvents are presented in **Table 4**.

Table 4. Photophysical properties of pyrido[2,3-*a*]carbazoles **5** (**a-q**)

			DCM		
Compounds	λ_{abs} (nm)	λ_{emi} (nm)	Φ_{fl}	$\Delta\nu$ (cm^{-1})	**ε** ($L\ mol^{-1}\ cm^{-1}$)
5a	393	459	0.51±0.04	3659	38790
5b	397	461	0.56±0.03	3497	37630
5c	395	461	0.41±0.055	3625	41120
5d	396	459	0.48±0.06	3466	39146
5e	400	462	0.53±0.05	3355	43010
5f	402	461	0.49±0.07	3184	43130
5g	399	464	0.44±0.04	3511	39790
5h	401	463	0.48±0.065	3339	41320
5i	392	451	0.28±0.03	3338	47670
5j	393	458	0.34±0.05	3611	45490
5k	396	454	0.24±0.075	3226	44660
5l	395	450	0.30±0.06	3094	41030
5m	397	458	0.33±0.045	3354	39980

5n	400	460	0.31±0.06	3261	40910
5o	389	455	0.47±0.05	3728	38940
5p	390	458	0.39±0.035	3807	39790
5q	389	463	0.43±0.05	4108	40150

It can be seen from **Table 4** that these compounds exhibit absorption maxima (λ_{abs}) in the UV-vis region (390-407 nm) and emission maxima (λ_{em}) yellow to red region (464-504 nm). It was observed that the absorption maxima of compounds **5**(**a**-**q**) exhibits two peaks in the UV region and near visible region which are due to the π-π* and n- π* transitions respectively. The shift of the absorption spectrum with solvent polarity observed for a solvatochromic compound is a well-known phenomenon. A change of solvents from DMF to DCM resulted in a little blue shift (2-9 nm) of the absorption maximum. **Fig. 6** represents normalized overlay absorption and emission spectra of the compounds **5** (**a**-**d**) in DCM solvent.

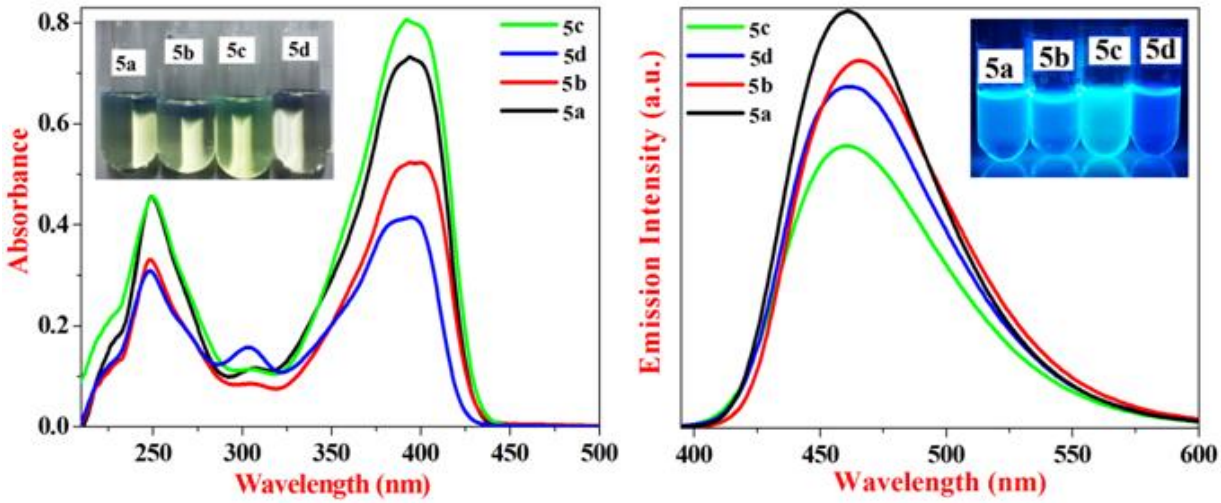

Fig. 6. Absorption (left) and fluorescence (right) spectra of **5** (**a**-**d**) in **DCM**

The maximal emission peaks of compounds **5** (**a**-**q**) are mainly located at about 464-504 nm with Stokes shift ranging from 2931-4729 cm^{-1}. The fluorescence peak displays a dramatic red shift compared to absorption maxima with increase in polarity of solvents. This is due to the more polar nature of the emitting state compared to ground state. Similar to absorption experiments, the emission spectra shifts to higher wavelengths with increasing solvent polarity (bathochromic shift) from DCM to DMF, conforming a π-π* transition. As an example, the

spectra registered for compound **5h** the emission wavelength at λ_{em} = 463 nm in the least polar solvent DCM is red-shifted by about 41 nm in DMF (λ_{em} = 504 nm). To check the emittive colour of these compounds, we illuminated our compounds in a UV transminallator and the results are represented in inset of respective images, which clearly indicate that the pyrido[2,3-*a*]carbazoles are highly emittive. The light pale yellow coloured solution (normal light) of the compounds emitted cyan colored fluorescence under UV light at 365 nm.

It is observed that the fluorescence spectra showed significant solvatochromism. An increase in the solvent polarity led to increase in the stoke shifts. This finding supports a highly polarized excited singlet state generated by the intramolecular charge transfer from the donor carbazole moiety to the acceptor cyano group. The large Stokes shifts are also indicative of the high polarizability of these systems due to the presence of both donor and acceptor groups coupled by a π-conjugated spacer.

It is intriguing to note that the presence of aryl/heteroaryl substituents at C-4 position make an impact on absorption and emission maxima. Both absorption spectra and emission spectra in better agreement with the increase of electron-withdrawing ability of the substituents. In particular, the thiophene group induces more red shift in both absorption and emission spectra and exhibited highest quantum yield value (Φ_{fl}=0.65).

The relative fluorescence quantum yield (φ_{fl}) of the pyrido[2,3-*a*]carbazoles was calculated using the following equation

$$\varphi_{fl} = \varphi_{ref} \frac{I_s A_{ref}}{I_{ref} A_s} \frac{n_s^2}{n_{ref}^2} \dots\dots\dots (1)$$

Where **A** is the absorbance at the excitation wavelengths, **I** is the integrated emission intensity, and **n** is the refractive indices of the solvents. The subscripts **s** and **ref** refer to the tested compounds and reference samples, respectivel . The quantum yield changed from 0.48 to 0.65 for compound **5h** with increasing solvent polarity. Compared to other solvents, DCM possesses the lowest dielectric constant and dipole moment, followed by CF, MeOH and DMF and the lowest quantum yield was also observed in DCM. That is, there was a correlation of quantum yield with dielectric constant and solvent polarity.

2.4. Fluorescence lifetime

Fluorescence life time (τ) is an intrinsic property of a fluorophore. The lifetime of photophysical processes vary significantly from tens of femtosecond for internal conversion to nanoseconds for fluorescence and microseconds or seconds for phosphorescence. Fluorescence lifetime can be considered as a state function because it is independent of wavelength of excitation, duration of light exposure, one-or multiphoton excitation, method of measurement, fluorescence intensity, fluorophore concentration and not affected by photobleaching. The Fluorescence life time measurements enables better understanding of excited state properties of molecules. Time resolved acquisition methods are used to determine the time decay of fluorophores. **Table.5** provides data from fluorescence decay analysis of compounds **5** (**a-q**) and the life time are relatively long from 7.14 to 9.13 ns. The lifetime is calculated using curve fitting algorithms, if the fit is monoexponential, the output provides a single fluorescent lifetime with goodness of fit parameters such as χ close to unity. Most decay curves can be well fitted with a single exponential value χ range 0.96 to 1.10 **(Fig.7** & **Fig.8**).

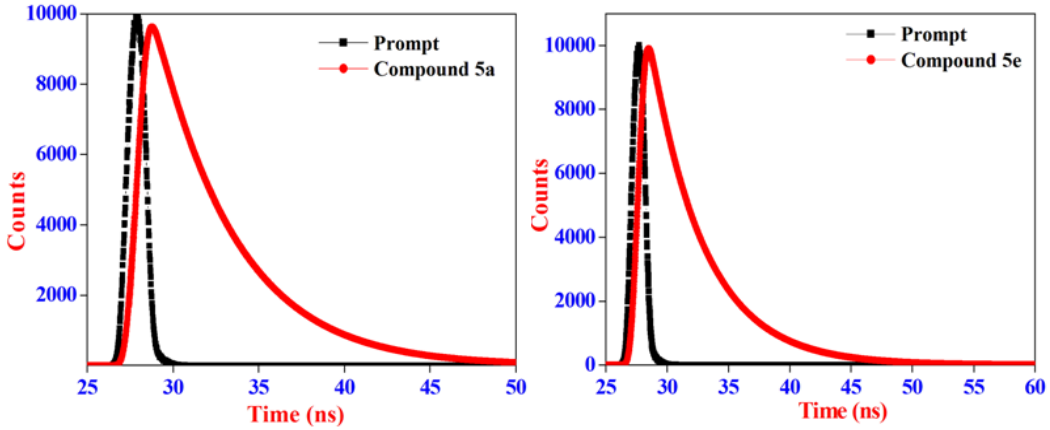

Fig. 7. Fluorescence decay curves of compounds **5a** & **5e**

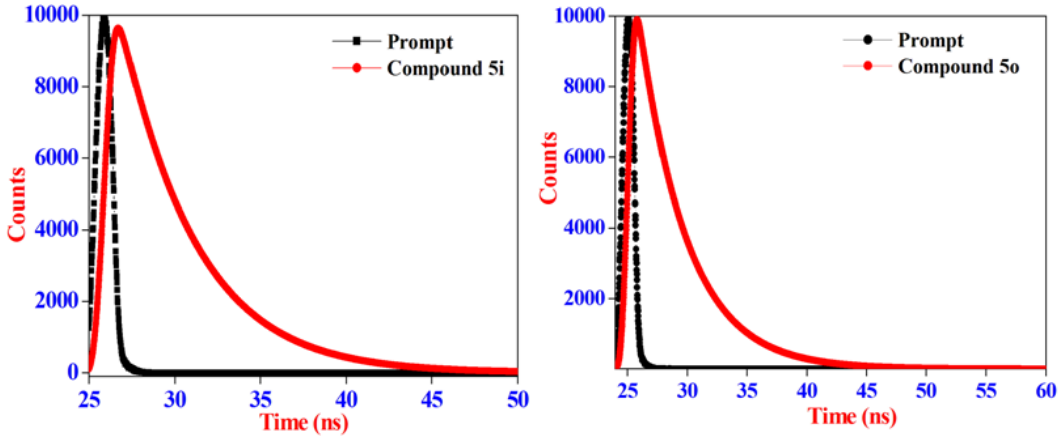

Fig. 8. Fluorescence decay curves of compounds **5i** & **5o**

Table 5. Fluorescence lifetime analysis of pyrido[2,3-*a*]carbazoles

Compounds	τ_1	a_1	τ_2	a_2	τ_1	a_3	τ_{avg} (ns)	χ
5a	2.23	0.018	4.45	-0.08	8.90	1.062	9.13	1.00
5b	2.27	0.021	3.98	0.019	8.78	0.960	8.55	1.02
5c	2.14	0.040	4.13	0.080	8.68	0.880	8.05	0.98
5d	1.98	0.080	3.75	0.020	7.67	0.900	7.14	0.97
5e	2.05	0.014	3.97	0.016	8.24	0.970	8.08	1.09
5f	2.13	0.019	4.25	0.001	8.45	0.980	8.32	1.06
5g	2.18	0.070	4.36	0.020	8.73	0.910	8.18	0.96
5h	1.89	0.006	3.76	0.009	7.89	0.980	7.79	1.01
5i	1.96	0.030	4.05	0.009	8.02	0.961	7.82	1.05
5j	2.03	0.022	3.74	0.011	8.11	0.967	7.93	1.10
5k	2.67	0.056	4.32	0.023	8.83	0.921	8.38	1.06
5l	2.11	0.032	3.59	0.009	7.97	0.951	7.67	1.03
5m	2.36	0.029	4.46	0.017	8.87	0.954	8.60	0.98
5n	2.10	0.043	4.25	0.014	8.38	0.943	8.06	1.01
5o	2.48	0.038	4.19	0.001	9.07	0.961	8.83	1.07
5p	2.26	0.031	4.45	0.012	8.86	0.957	8.60	0.99
5q	1.95	0.042	3.56	0.007	8.75	0.951	8.42	1.03

$\langle\tau_{avg}\rangle = \tau_1 a_1 + \tau_2 a_2 + \tau_3 a_3$

2.5. DFT calculations

In order to understand the electronic properties of the synthesized compounds, density functional theory (DFT) calculations were carried out using the Gaussian 09 program package. At first, the molecular structures were optimized to find the ground state structures through M06-2X/6-31G** level of theory. Since significant improvement of M06-2X, a DFT functional for electronic calculations reported by E.G. Hohenstein *et al*.,[39] for this, we used corresponding coordinates extracted from the crystal lattice using Mercury software. The geometrical parameters (bond length and angle) of the optimized structures are not much varying (approximately same) with experimental results and the structures were clearly showed in **Fig. 9**. The UV- visible absorption spectra of the π-conjugated organic molecules originates from π-π* and n-π* transitions. These transitions involve electron transfer between the Highest Occupied Molecular Orbitals (HOMO) and Lowest Unoccupied Molecular Orbitals (LUMO), called the Frontier Molecular Orbitals (FMO). The comparison of these HOMO and LUMO values and energy gap for selective compounds were visualized in **Fig. 10** using M06-2X/6-31G** level of theory with gas phase medium. This figure clearly shows the localized electron density region at HOMO and LUMO position for the corresponding molecules. The results point out that, the compound **5h** bearing thiophene moiety exhibited lowest value of energy gap (5.469eV) compared with other compounds due to higher overlapping of HOMO-LUMO orbital's and displayed high conducting property. This compound also showed bathochromic shift in emission spectra and high fluorescence quantum yield. Furthermore we compared these results with more level of theories such as M06-2X, M05-2X, M06-HF and B3LYP with the same basis set 6-31G** with gas phase medium (**Table 6**). By comparing all level of theories, energy gap values are observed with around 5eV except in the case of B3LYP/6-31G** which is around 3eV. From this, it was observed that the results of B3LYP functional are comparable with the experimental maximum absorption wavelength of all five molecules. Furthermore, we have the experimental maximum absorption wavelength for different solvent medium (DCM, CF, MeOH and DMF). In order to compare the energy gap, we analyzed with different solvent phase mediums at B3LYP/6-31G** level of theory. These results also well correlated with experimental results of maximum absorption wavelength in eV (changes upto only ˷0.4 eV). The results were listed out in **Table 7** for DCM, CF, MeOH and DMF medium.

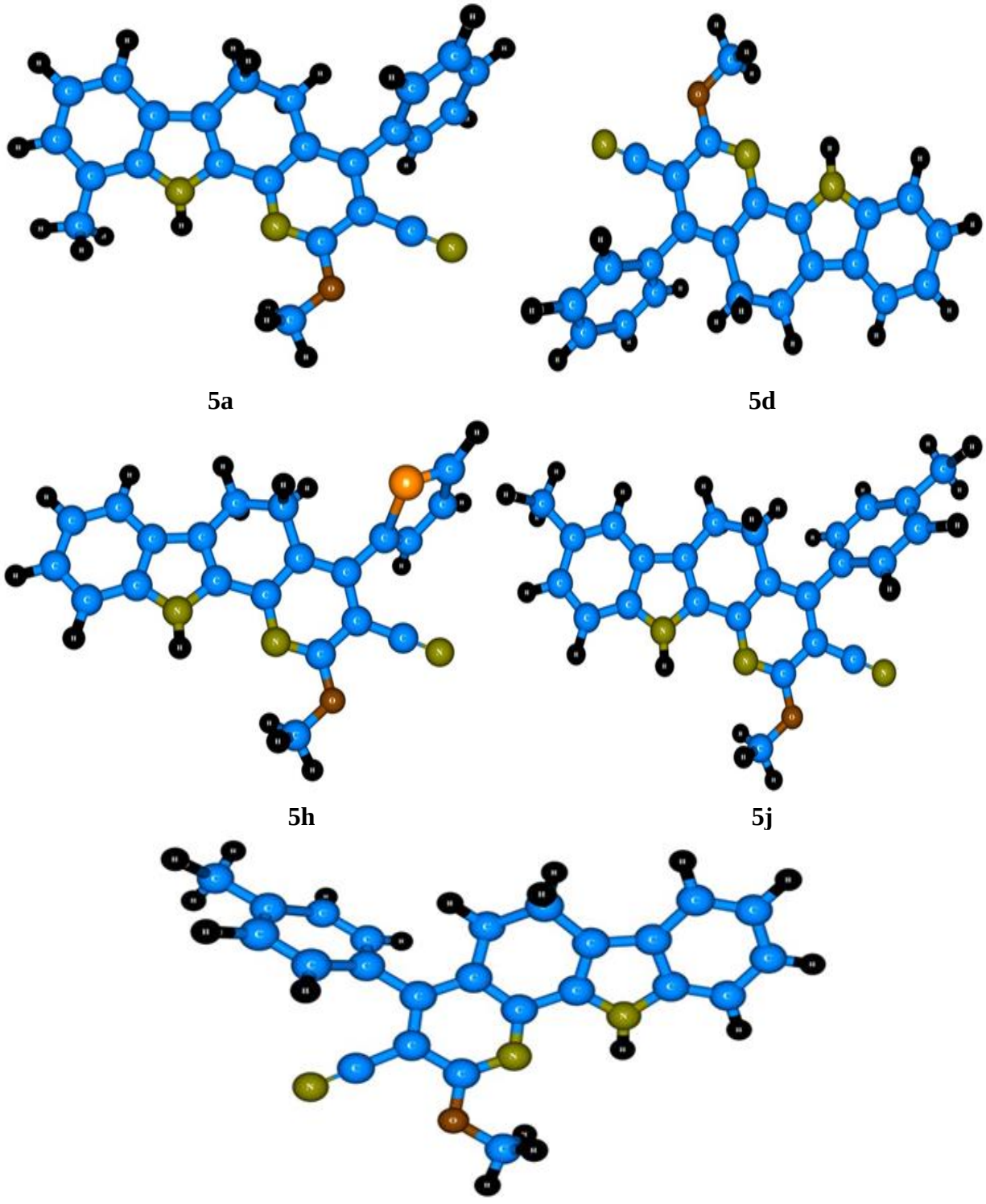

Fig. 9. Optimized structures of **5a**, **5d**, **5h**, **5j** and **5k** using M06-2X/6-31G** level of theory

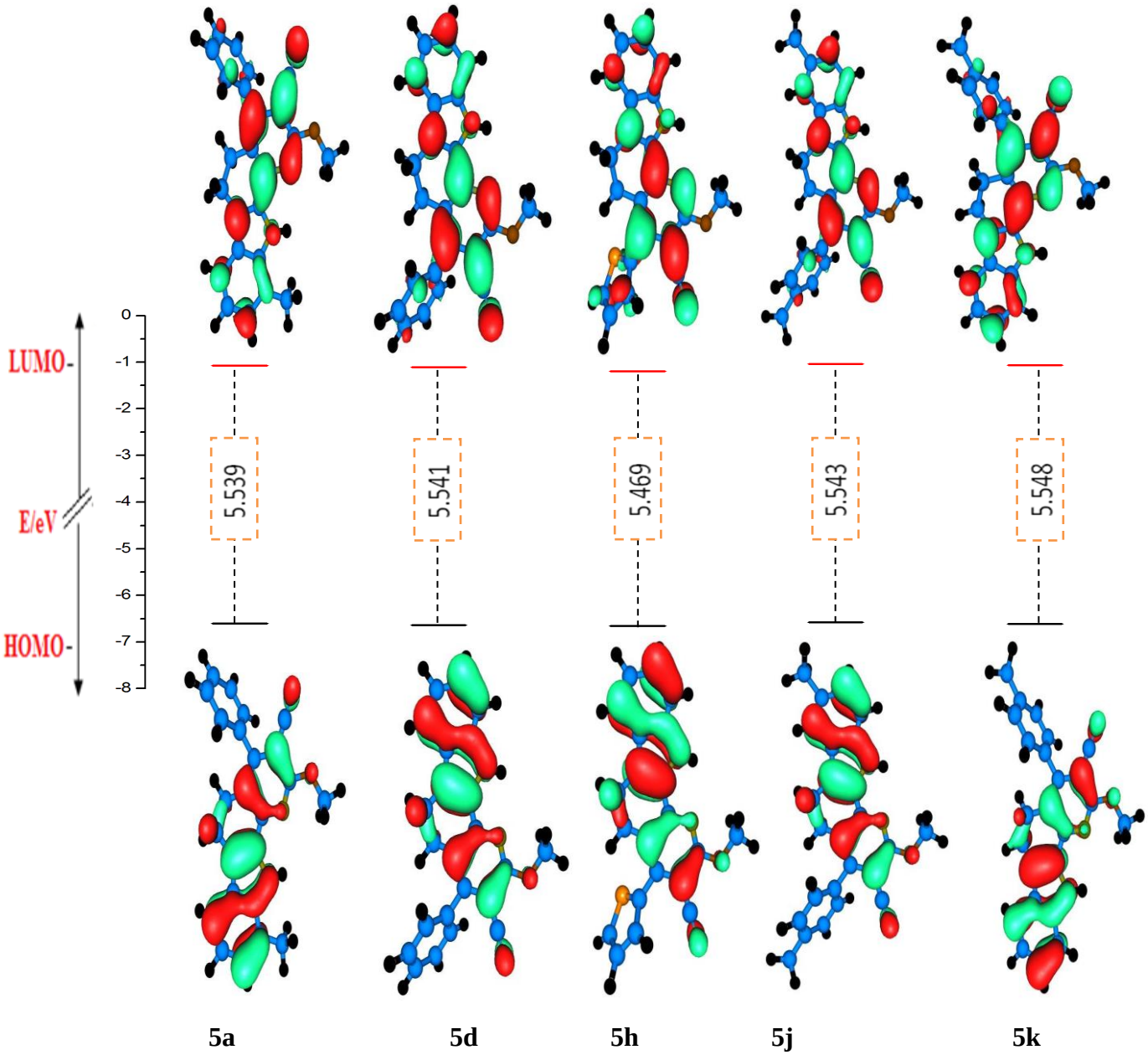

Fig. 10. FMO energy levels of compounds **5a**, **5d**, **5h**, **5j** and **5k** calculated using M06-2X/6-31G** level of theory.

Table 6. Electrochemical properties of the compounds **5a, 5d, 5h, 5j** and **5k** calculated with gas phase medium by FMO calculation.

Molecule	M052X	M062X	M06HF	B3LYP

	HOMO Ev	LUMO eV	Band gap	HOMO eV	LUMO eV	Band gap	HOMO eV	LUMO eV	Band gap	HOMO eV	LUMO eV	Band gap
5a	-6.658	-1.003	5.655	-6.599	-1.060	5.539	-8.147	0.005	8.153	-5.384	-1.794	3.589
5d	-6.695	-1.038	5.658	-6.635	-1.094	5.541	-8.186	-0.026	8.159	-5.420	-1.830	3.590
5h	-6.714	-1.132	5.582	-6.654	-1.185	5.469	-8.210	-0.127	8.082	-5.436	-1.914	3.522
5j	-6.627	-0.968	5.660	-6.569	-1.027	5.543	-8.122	0.036	8.157	-5.350	-1.755	3.595
5k	-6.664	-0.999	5.664	-6.605	-1.057	5.548	-8.160	0.007	8.167	-5.385	-1.790	3.595

Table 7. Electrochemical properties of the compounds **5a, 5d, 5h, 5j** and **5k** in DCM, $CHCl_3$, MeOH and DMF in phase medium using B3LYP/6-31G** level of theory by FMO calculation.

Molecule	DCM			$CHCl_3$			MeOH			DMF		
	HOMO Ev	LUMO eV	Band gap	HOMO eV	LUMO eV	Band gap	HOMO eV	LUMO eV	Band gap	HOMO eV	LUMO eV	Band gap
5a	-5.420	-1.896	3.524	-5.413	-1.878	3.535	-5.427	-1.912	3.514	-5.427	-1.913	3.514
5d	-5.449	-1.920	3.529	-5.443	-1.903	3.540	-5.455	-1.936	3.519	-5.455	-1.936	3.519
5h	-5.458	-1.997	3.460	-5.452	-1.981	3.471	-5.464	-2.012	3.451	-5.464	-2.013	3.451
5j	-5.408	-1.877	3.532	-5.397	-1.855	3.542	-5.418	-1.897	3.521	-5.418	-1.898	3.520
5k	-5.433	-1.899	3.534	-5.424	-1.879	3.544	-5.441	-1.917	3.524	-5.441	-1.918	3.523

3. Conclusions

In conclusion, we have devised a versatile, convenient, and efficient approach to construct the structurally diverse and fluorescent pyrido[2,3-*a*]carbazoles via four-component one-pot reaction of 2,3,4,9-tetrahydro-1*H*-carbazole, malononitrile and aldehydes through domino Knoevenagel condensation in the presence of NaOEt in MeOH. The advantage of operational simplicity, generality, fairly fast reaction times, economic viability, generality, atom-economy make this protocol a very efficient alternative to literature methods. The synthesized compounds were subjected to photophysical studies and DFT theoretical evaluation. The photophysical properties of the synthesized compounds were systematically studied in four organic solvents having different polarities. The UV absorption and fluorescence emission of compounds were found to be solvent dependent and showed positive solvatochromic behavior in both absorption and emission spectra. Fluorescence quantum yield (φ_{fl}) and Stokes shift ($\Delta\nu$) are strongly influenced by the polarity of the solvents. Fluorescence decays of compounds 5 (a-q) in methanol fitted with monoexponential functions indicating emission from the singlet excited state in all cases. The synthesized compounds were subjected to DFT computational study using different functional theories. The calculated HOMO and LUMO energies show that charge

transfer occurs within the molecule. The photophysical properties displayed by the synthesized pyrido[2,3-*a*]carbazoles conclude that these compounds are promising candidates for fluorescent probes and fluorescent makers due to their strong fluorescence properties. Further scope of the methodology has been exploited and various biological application studies are currently underway in our laboratory.

Acknowledgments

We would like to thank the University of Mysore, for NMR data. X-ray diffraction was funded by University of Bristol, United Kingdom. Financial support from "UGC-Emeritus fellowship" (Award NO.F.6-6/2015-17/EMERITUS-2015-17-OBC-7410/(SAII)) for research, Dr. K. J. Rajendra Prasad gratefully acknowledged. We also thank UGC-RGNF, New Delhi for further financial assistance and successful completion of this work.

Supplementary data

CIF files for the compounds **5a, 5d, 5h, 5j** and **5k** have been deposited with the Cambridge Crystallographic Data Centre as CCDC numbers 1498651-1498655. Copies of the data can be obtained, free of charge, on application to CCDC, 12 Union Road, Cambridge, CB2 1EZ, UK. [Fax: +44 (0) 1223 336033 or e-mail: deposit@ccdc.cam.ac.uk. Spectral data of all the compounds are associated with this article will be available as supporting information.

Notes and references

1 (*a*) M. Fox, *Chem. Rev*., 1992, **92**, 365-368; (*b*) P. Sarder, D. Maji and S. Achilefu, *Bioconjugate Chem*., 2015, **26**, 963-974.

2 Z. Xia, Z. Zhang, J. Su, Q. Zhang, K. Fung, M. Lam, K. Li, W. Wong, K. Cheah, H. Tian and C. Chen, *J. Mater*. *Chem*., 2010, **20**, 3768-3774.

3 (*a*) J. R. Lakowicz, *Plenum Press, New York*, 1994, **4**, 501-504; (*b*) X. Fei and Y. Gu, *Prog. Nat. Sci.*, 2009, **19**, 1-7.

4 (*a*) B. Balaganesan, S. Wen and C. Chen, *Tetrahedron Lett*., 2003, **44**, 145-147; (*b*) S.K. Pathak, R.K. Gupta, S. Nath, D.S.S. Rao, K. Prasad, A.S. Achalkumar, *J Mater Chem. C*, 2015, **3**, 2940-2952.

5 (*a*) G. Yu, J. Gao. J. Hummelen, F. Wudl and A. Heeger, *Science*, 1995, **270**, 1789-1791; (*b*) S. Hattori, Y. Wada, S. Yanagida, S. Fukuzumi, *J. Am. Chem. Soc.*, 2005, **26**, 9648–9654; (*b*) S. Westenhoff, I.A. Howard, J.M. Hodgkiss, K.R. Kirov, H.A. Bronstein, C.K. Williams, N.C. Greenham, R.H. Friend, *J. Am. Chem. Soc.* 2008, **130**, 13653–13658; (*c*) J.F. Yin, J.G. Chen, Z.Z. Lu, K.C. Ho, |*J. Org. Chem.*, 2011, **76**, 4444–4456.

6 (*a*) H. Gold and K. Venkataraman, *Academic press, New York*, 1971, 535-679; (*b*) K. Hunger, Industrial dyes. Weiheim, Germany: Wiley-VCH, 2003; pp 569–577.

7 W. Rettig, *Angew, Chem. Int. Ed*., 1986, 25, 971-988.

8 A. C. Arias, J. D. MacKenzie, I. McCulloch, J. Rivnay and A. Salleo, *Chem. Rev*., 2010, 110, 3-24.

9 K. M. Rahulan, S. Balamurugan, K. S. Meena, G. Y. Yeap and C. C. Kanakam, *Opt. Laser. Technol*., 2014, 56, 142-145.

10 Z. R. Grabowski, K. Rotkiewicz and W. Rettig, *Chem. Rev*., 2003, 103, 3899-4302.

11 (*a*) R. P. Haugland, The Handbook A guide to Fluorescent Probes and Labeling Technologies, 10 ed., *Invitrogen*, 2005; (*b*) S. Achelle, J.R. Lopez, F. Bures and F.R. Guen, *Dyes Pigm*., 2015, **121**, 305-311; (*c*) K. Hoffert, R.J. Durand, S. Gauthier, F.R. Guen and S. Achelle, *Eur. J. Org. Chem*., 2017, 523-529.

12 H. N. Kim, Z. Guo, W. Zhu, J. Yoon and H. Tian, *Chem. Soc. Rev*., 2011, 40, 79-93.

13 G. S. He, L-S. Tan, Q. Zheng and P. N. Prasad, *Chem. Rev*., 2008, 108, 1245-1330.

14 Z. Li, Q. Li and J. Qin, *Polym*. Chem., 2011, 2, 2723-2740.

15 J. X. Yang, X. T. Tao, C. X. Yuan, Y. X. Yan, L. Wang, Z. Liu, Y. Ren and M. H. Jiang, *J. Am. Chem. Soc*., 2005, 127, 3278-3279.

16 R. M. Adhikari, R. Mondal, B. K. Shah and D. C. Neckers, *J. Org. Chem*., 2007, 72, 4727-4732.

17 H. Yu, S. M. Zain, I. V. Eigenbrot and D. Phillips, *Chem. Phys. Lett*., 1993, 202, 141-147.

18 R. Howell, A. G. Taylor, D. Phillips, *Chem. Phys. Lett*., 1992, 188, 119-125.

19 Molecular Association Including Molecular Complexes; Foster, R., Ed.; Academic Press: *New York, NY, USA*, 2, 1979.

20 S. M. Budy, S. Suresh, B. K. Spraul and D. W. Smith, *J. Phys. Chem. C*, 2008, 112, 8099-8104.

21 S. J. Su, H. Sasabe, T. Takeda and J. Kido, Chem. Mater., 2008, 20, 1691-1693.

22 S. Dailey, M. Halim, E. Rebourt, L. E. Hoursburgh, I. D. W. Samuel and A. P. Monkman, *J. Phys. Condens. Matter*., 1998, 10, 5171-5178.

23 J. M. Raimundo, P. Blanchard, P. Frere, N. Mercier, I. Ledoux Rak, R. Hierle and J. Roncali, *Tetrahedron Lett*., 2001, 42, 1507-1510.

24 A. K. Y. Jen, Y. M. Cai, P. V. Bedworth and S. R. Marder, *Adv. Mater*., 1997, 9, 132-135.

25 V. P. Rao, Y. M. Cai and A. K. Y. Jen, *J. Chem. Soc. Chem. Commun*., 1994, 14, 1689-1690.

26 M. Q. He, T. M. Leslie, J. A. Sinicropi, S. M. Garner and L. D. Reed, *Chem. Mater*., 2002, 14, 4669-4675.

27 J. Roncali, *Chem. Rev*., 1997, 97, 173-205.

28 J. M. Tour, *Chem. Rev*., 1996, 96, 537-553.

29 H. Xu, M. Zhang, A. Zhang, G. Deng, P. Si, H. Huang, C. Peng, M. Fu, J. Liu, L. Qiu, Z. Zhen and S. Bo, *Dyes Pigm*., 2014, 102, 142-149.

30 (a) T. Indumathi, A. Muthushankar, P. Shanmugavel and K. J. Rajendra Prasad. *Med. Chem. Commun*., 2013, 4, 450-455: (b) M. Sridharan, L. K. Beagle, M. Zeller and K. J. Rajendra Prasad, *J. Chem. Res*., 2008, 572-577.

31 Bruker-AXS SAINT V8.27B Madison, Wisconsin.

32 G. M. Sheldrick, SADABS V2012/1, University of Göttingen, Germany.

33 (a) L. Palatinus, G. Chapuis, *J. Appl. Cryst,*. 2007, 40 786-790; (b) L. Palatinus, A. Lee van der, *J. Appl. Cryst*. 2008, 41, 975-984; (c) L. Palatinus, S. J. Prathapa, S. Smaalen van, *J. Appl. Cryst*., 2012, 45, 575-580.

34 G. M. Sheldrick, Acta Cryst. A. 64 (2008) 112.

35 O. V. Dolomanov, L. J. Bourhis, R. J. Gildea, J. A. K. Howard, H. Puschmann, *J. Appl. Cryst.* 2009, 42, 339-341.

36 D. Magde, R. Wong, P. G. Seybold, *Photochem. Photobiol*., 2002, 75, 327–334.

37 M. Beija, C. A. M. Afonso, Jose M. G. Martinho, *Chem. Soc. Rev*., 2009, 38, 2410–2433.

38 P. D. Sahare, V. K. Sharma, D. Mohan, A. A. Rupasov, *Acta Part-A.,* 2008, 69, 1257–1264.

39 E. G. Hohenstein, S. T. Chill and C. D. Sherrill, *J. Chem. Theory Comput*., 2008, 4, 1996–2000.

40 Gaussian 09, Revision B.01, M. J. Frisch, G. W. Trucks, H. B. Schlegel, G. E. Scuseria, M. A. Robb, J. R. Cheeseman, G. Scalmani, V. Barone, B. Mennucci and G.A. Petersson, et al., Gaussian, Inc., Wallingford CT, 2010.

41 X. Shang, Y. Li, Q. Zhan and G. Zhang, *New J. Chem*., 2016, 40 1111–1117.